

## Geochemistry of sandstone-mudstone suites of the Tipam Sandstone Formation, Surma Basin, Bangladesh

Dhiman Kumer ROY<sup>1</sup>, Md. Mostafizur RAHMAN<sup>1</sup>, Syed Samsuddin AHMED<sup>1</sup>, Ismail HOSSAIN<sup>1,2</sup> and Sarmin AKHTER<sup>1</sup>

### Abstract

The geochemical study of the Tipam Sandstone Formation in the Surma Basin of the Bengal Basin reveals the tectonic setting, provenance in relation to composition, weathering history in source area and the climatic condition during deposition. The geochemical characteristics as shown by CaO-Na<sub>2</sub>O-K<sub>2</sub>O, Fe<sub>2</sub>O<sub>3</sub>-MgO-TiO<sub>2</sub> and CaO-Na<sub>2</sub>O-K<sub>2</sub>O plots indicate with higher ratios of SiO<sub>2</sub>/Al<sub>2</sub>O<sub>3</sub>, K<sub>2</sub>O/Na<sub>2</sub>O. This characteristics and Chemical Index of Alteration (CIA) highly support that the source rocks were dominated by old upper crustal granite and quartz monzonite. They also include recycled sedimentary rocks of the old continental foundation of active tectonic setting that subjected intensive weathering. Harker variation diagrams show positive correlation of K<sub>2</sub>O and Na<sub>2</sub>O, and negative correlation of CaO, Fe<sub>2</sub>O<sub>3</sub> and MgO with SiO<sub>2</sub>. This phenomenon indicates that the concentration of K<sub>2</sub>O and Na<sub>2</sub>O increase with increasing SiO<sub>2</sub> whereas CaO, Fe<sub>2</sub>O<sub>3</sub> and MgO decrease with increasing SiO<sub>2</sub>. This supports the derivation of the sediment from felsic igneous rocks i.e. from granitic rocks. SiO<sub>2</sub> content versus K<sub>2</sub>O/Na<sub>2</sub>O as well as SiO<sub>2</sub>/Al<sub>2</sub>O<sub>3</sub> versus K<sub>2</sub>O/Na<sub>2</sub>O diagrams, K<sub>2</sub>O/Na<sub>2</sub>O ratio and (Fe<sub>2</sub>O<sub>3</sub>+MgO)-Na<sub>2</sub>O-K<sub>2</sub>O triangular plot indicate that the sediments were deposited in a basin along passive margin tectonic setting.

**Key words:** Geochemistry, Tipam Sandstone Formation, Surma basin, Provenance, Paleoclimate

### Introduction

The present work has been made to focus on the nature of the source terrane, provenance, tectonic setting of depositional basin, paleoclimate and weathering history of the Tipam Sandstone Formation in the Surma Basin, Bangladesh on the basis of

geochemical investigations of sandstone-mudstone suites. Provenance is critical for deciphering the tectonic history of ancient basins and has been applied to both terrane analysis and basin analysis. Provenance is also an important factor for finding petroleum reservoirs system within sedimentary basins.

The studied area is bounded within latitudes from 24°83' to 24°88'N and longitudes from 92°07' to 92°11' E (Fig. 1) and is situated at about 30 km northeast of Sylhet town. The area includes Lalakhil Tea garden, Kamrangi, Nichinpur, Putikhil and Dighral areas of Jaintiapur upazila, which are in the northeastern part of Sylhet district, Bangladesh. The rocks of the Tipam Sandstone Formation are mainly composed of sandstones with intermittently alternation of sandstones and shales. On the basis of lithology, these rocks have been divided into the Lower Tipam Sandstone, the Middle Tipam Sandstone and the Upper Tipam Sandstone. The Lower Tipam Sandstone consists of yellowish brown to dark brown sandstone and occasionally of reddish brown conglomeratic sandstone, siltstone, mudstone and clay. Mudstone and clay, minor lithology are composed of gray, occasionally grayish black, massive clay or mudstone. The Middle Tipam Sandstone consists of grey colored parallel laminated silty shale with alternation of grayish white ripple laminated siltstone and fine-grained sandstone. The Upper Tipam Sandstone is composed of medium to very fine-grained sandstones with parallel laminated to ripple cross-laminated siltstone, laminated silty shale and unsullied shale. The thickness of the Late Mesozoic and Cenozoic strata in the Surma Basin ranges from about 13 to 17 km (Evans, 1964; Hiller and Elahi, 1984) and much of these strata (Formations) are included Neogene age (Table 1).

The geochemistry of the sandstone and shale is a powerful tool to provide information about the provenance, tectonic setting, paleoclimate and weathering history. Recent and ancient detritus have been used to infer them by many workers (Condie, 1976; Le Maitre, 1976; Potter, 1978; Blatt *et al.*, 1980;

<sup>1</sup> Department of Geology and Mining, University of Rajshahi, Rajshahi-6205, Bangladesh.

<sup>2</sup> Earth Evolution Sciences, Graduate School of Life and Environmental Sciences, University of Tsukuba, Ibaraki 305-8572, Japan

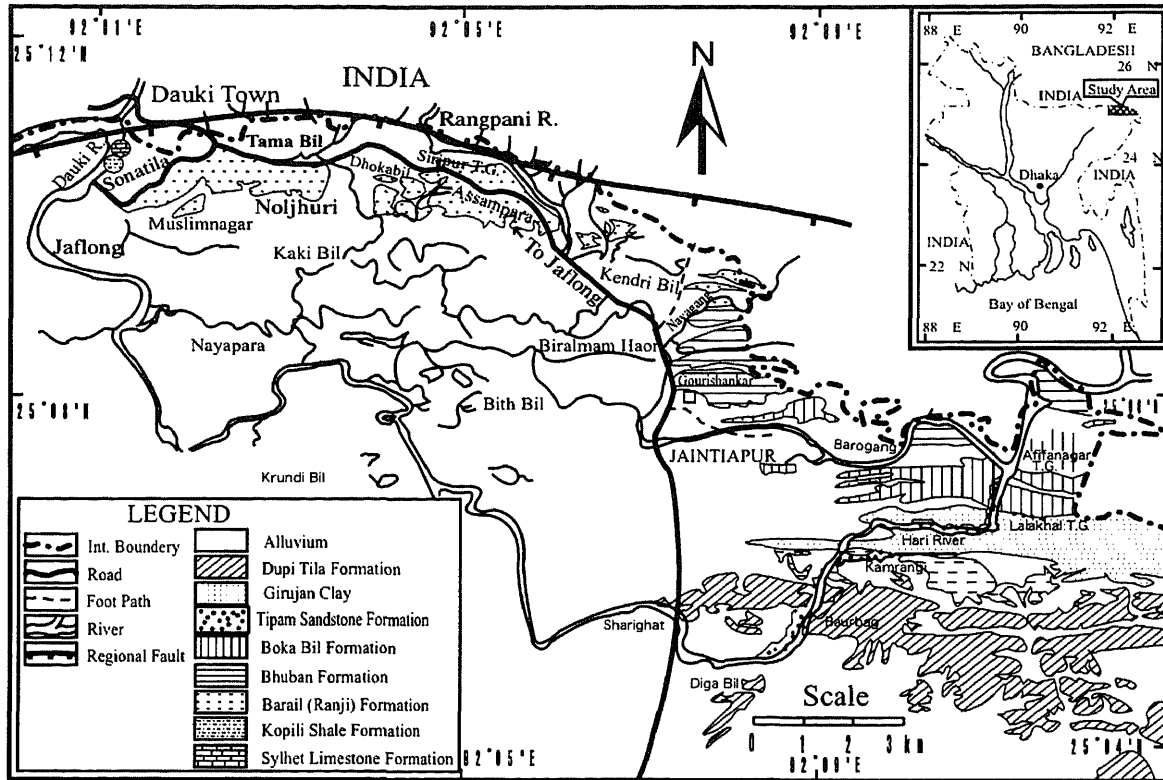


Fig. 1 Geological map of the study area showing the exposed Tertiary rock sequence.

Table 1. The stratigraphic succession of the Sylhet Trough (after Khan *et al.*, 1988).

Age	Group	Formation
Plio-Pleistocene	Dihing Group	Upper
	Dupi Tila Group	Lower
Pliocene	Tipam Group	Girujan Clay
		Tipam Sandstone
Pliocene Miocene	Surma Group	Boka Bil
		Bhuban
Oligocene	Barail Group	Renji
		Jenam
		Laisong
Eocene	Jaintia Group	Kopili
		Sylhet Limestone
		Cherra.

Bhatia, 1983; Hiscott, 1984; Bhatia and Crook, 1986; Roser and Korsch, 1986, 1988; Suttner and Dutta, 1986; Nesbitt and Young, 1984; McLennan *et al.*, 1993). Roser and Korsch (1986) used the diagrams of  $\text{SiO}_2$  vs.  $\text{K}_2\text{O}/\text{Na}_2\text{O}$  and  $\text{SiO}_2/\text{Al}_2\text{O}_3$  vs.  $\text{K}_2\text{O}/\text{Na}_2\text{O}$  of published data from sandstone-mudstone suites to discriminate passive margin (PM), active continental margin (ACM), oceanic island arc (ARC) settings.

### Geologic Setting

Tectonically the studied area in the Sylhet Trough, a sub-basin of the Bengal Basin in northeastern Bangladesh, is a complex province of the Bengal Basin. The Bengal basin lies on the eastern side of the Indian subcontinent and occupies most of Bangladesh and west Bengal of India as well as part of the Bay of Bengal (Alam, 1989). The Shillong Plateau bound

this Trough on the north, on the east and southeast by the Chittagong Tripura fold belt of the Indo-Burman ranges and on the west by the Indian Shield Platform, which is open to the south and southwest to the main part of the Bengal Basin (Johnson and Alam, 1991). The Surma Basin had its origin in the collision of India with Eurasia and Burma, building the extensive Himalayan and Indo-Burman ranges and thereby loading the lithosphere to form flanked sedimentary basins (Uddin and Lundberg, 1998). Johnson and Alam (1991) proposed that the Sylhet Trough has undergone a complex evolution recording the transition from a passive, rifted continental margin to a foreland basin on the margins of two mobile belts. The Sylhet Trough formed a portion of the foreland basin of the Himalaya orogen and the Indo-Burman Ranges (active continental margin). The Dauki fault system with huge vertical displacements represents the contact between the Surma Basin and Shillong Plateau (Hiller and Elahi, 1984; Johnson and Alam, 1991; Reimann, 1993). Johnson and Alam (1991) suggested that the Tipam Sandstone Formation has been formed in a bedload-dominated (probably braided) fluvial system. The grain size, shape, facies sequence, association, paleocurrent pattern and paleoslope indicates single source of sediment and the sediments deposited in a heavily loaded, low sinuous and high sloped ( $16^{\circ}$ – $22^{\circ}$ ) braided river system (Roy *et al.*, 2006).

### Sample and analytical methods

A number of sandstone and shale samples were collected from the Tipam Sandstone Formation along the Hari River section, in the Surma Basin, Bangladesh. Fresh 15 sandstone and 8 shale samples were randomly selected for the analysis of major element composition ( $\text{SiO}_2$ ,  $\text{Al}_2\text{O}_3$ ,  $\text{K}_2\text{O}$ ,  $\text{Na}_2\text{O}$ ,  $\text{CaO}$ ,  $\text{Fe}_2\text{O}_3$ ,  $\text{MgO}$ ,  $\text{P}_2\text{O}_5$ ,  $\text{TiO}_2$  and  $\text{MnO}$  wt%). These samples were collected from Lower Tipam (LTS), Middle Tipam (MTS) and Upper Tipam Sandstone (UTS) Formation: ten samples of Lower Tipam, five samples of Middle Tipam and eight samples of Upper Tipam. First the samples were dried at  $110^{\circ}$ – $120^{\circ}\text{C}$ . Then dried samples were heated for two hours at  $950^{\circ}\text{C}$  endothermic peak temperature. Moisture loss was determined in the Soil Research Development Institute (SRDI), Rajshahi, Bangladesh. Then the crushed samples were used to determine the major element composition by XRF. Analyses were carried out with standard curves based on International Rock Standards (model Philips-2000) in the Glass and Ceramic Division of Bangladesh Council of Science and Industrial Research (BCSIR), Dhaka, Bangladesh.

## Results

### 1. Major element geochemistry of sandstone

The major element compositions of 15 representative sandstone samples were selected for analyses (Table 2). Correlation between the elements is given in Table 3. The  $\text{SiO}_2$  content varies from 40.1 to 75.8 wt% with an average of 67.9 wt%. It shows negative correlation with  $\text{Fe}_2\text{O}_3$ ,  $\text{TiO}_2$ ,  $\text{CaO}$ ,  $\text{MgO}$ ,  $\text{MnO}$  and  $\text{ZrO}_2$  contents but significant with  $\text{CaO}$  ( $r = -0.93$ ) and  $\text{MnO}$  ( $r = -0.83$ ), whereas positive correlation exists with  $\text{Al}_2\text{O}_3$ ,  $\text{Na}_2\text{O}$  and  $\text{K}_2\text{O}$  contents.  $\text{Al}_2\text{O}_3$  varies from 9.0 to 21.4 wt%, with an average of 15.1 wt%. It shows high positive correlation only with  $\text{K}_2\text{O}$  ( $r = 0.854$ ) and negative correlation significantly with  $\text{CaO}$  ( $r = -0.65$ ) and  $\text{MgO}$  ( $r = -0.67$ ). The studied sandstones contain small amount of  $\text{Na}_2\text{O}$  (0.1 to 1.0%), with an average of 0.6 wt%. It shows negative correlation with  $\text{K}_2\text{O}$  ( $r = -0.57$ ). The maximum value of  $\text{K}_2\text{O}$  is 3.2 wt% and the minimum is 1.9 wt% with the average value of 2.3 wt%. It shows positive correlation with  $\text{SiO}_2$ ,  $\text{Al}_2\text{O}_3$  and  $\text{TiO}_2$ . The total iron, expressed in  $\text{Fe}_2\text{O}_3$ , attains maximum value of 11.8 wt% and minimum of 3.5 wt% with an average of 5.4 wt%. The  $\text{TiO}_2$  content ranges from 0.5 to 0.9 wt% with average of 0.6 wt%. It shows negative correlation with  $\text{MnO}$  ( $r = -0.85$ ).  $\text{CaO}$  content varies from 0.3 to 36.4 wt% with average contents of 5.0 wt%. It shows positive correlation with  $\text{MgO}$  ( $r = 0.60$ ) and  $\text{MnO}$  ( $r = 0.88$ ). The  $\text{MgO}$  content varies from 0.4 to 2.6 wt% with an average of 1.4 wt%. It shows negative correlation with  $\text{SiO}_2$  and  $\text{Al}_2\text{O}_3$ .  $\text{MnO}$  occurs in minor amounts, and shows maximum value of 1.0 wt% and minimum value of 0.1 wt% with an average content of  $\text{MnO}$  is 0.4 wt%.

### 2. Major element geochemistry of shale

Eight representative shale samples were selected for the major element analyses (Table 4). Correlation between the elements is given in Table 5. The  $\text{SiO}_2$  content varies from 27.8 to 63.9 wt% with an average of 55.7 wt%. It shows positive correlation with  $\text{Al}_2\text{O}_3$ ,  $\text{Na}_2\text{O}$ ,  $\text{K}_2\text{O}$  and  $\text{ZrO}_2$ . Well correlations are with  $\text{Al}_2\text{O}_3$  ( $r = 0.96$ ),  $\text{Na}_2\text{O}$  ( $r = 0.86$ ),  $\text{K}_2\text{O}$  ( $r = 0.90$ ) and  $\text{TiO}_2$  ( $r = 0.89$ ). The  $\text{Al}_2\text{O}_3$  content varies from 7.4 to 20.6 wt% with an average of 16.8 wt%. It shows high positive correlation with  $\text{K}_2\text{O}$  ( $r = 0.98$ ),  $\text{Na}_2\text{O}$  ( $r = 0.86$ ) and  $\text{TiO}_2$  ( $r = 0.96$ ) whereas negative correlation exists with  $\text{CaO}$  ( $r = -0.88$ ). Low  $\text{Na}_2\text{O}$  content (0.2 to 0.6 wt%, with an average of 0.6 wt%) occurs in shale. It shows positive correlation with  $\text{K}_2\text{O}$  ( $r = 0.84$ ).  $\text{K}_2\text{O}$  content varies from 1.2 to 3.8 wt% with an average of 2.9 wt%. It shows high positive correlation with  $\text{TiO}_2$  ( $r = -0.96$ ). The total iron, expressed in  $\text{Fe}_2\text{O}_3$ , attains

Table 2. Chemical composition (wt%) of sandstone, Tipam Sandstone Formation.

SAMPLE NO	SiO <sub>2</sub>	Al <sub>2</sub> O <sub>3</sub>	Na <sub>2</sub> O	K <sub>2</sub> O	Fe <sub>2</sub> O <sub>3</sub>	TiO <sub>2</sub>	CaO	MgO	MnO	P <sub>2</sub> O <sub>5</sub>	BaO	ZrO <sub>2</sub>	Loss	Total
LTS-1	69.781	21.444	0.115	2.736	3.721	0.647	0.333	0.386	0.085	-	0.132	0.018	0.60	99.998
LTS-2	71.747	19.112	0.138	2.881	3.615	0.553	0.350	0.403	-	-	-	-	1.20	99.999
LTS-3	73.833	15.426	0.819	2.276	3.860	0.496	1.096	0.646	0.077	0.154	0.111	-	1.20	99.999
LTS-4	72.145	13.503	0.804	1.928	7.244	0.649	1.505	1.092	0.287	0.417	-	0.025	0.40	99.999
LTS-5	63.695	16.999	0.387	2.536	11.753	0.677	0.688	0.610	0.242	0.226	0.159	-	0.20	98.172
LTS-6	40.101	9.030	0.508	1.905	5.657	0.611	36.346	2.614	1.029	-	-	-	0.80	98.606
LTS-7	75.770	12.081	0.925	2.015	3.829	0.475	1.762	2.114	-	0.202	-	0.022	0.20	99.4
LTS-8	59.348	11.175	0.774	1.926	5.212	0.926	15.695	2.272	0.409	0.226	-	0.038	0.40	98.401
LTS-9	73.318	14.158	0.758	2.004	5.940	0.568	1.305	1.210	0.198	-	-	-	1.20	100.704
LTS-10	71.336	14.266	1.038	2.066	4.307	0.588	1.642	1.550	-	0.234	-	0.020	0.80	97.857
MTS-1	71.738	15.209	0.914	2.243	4.901	0.601	1.562	1.439	0.244	0.190	0.125	0.032	0.80	99.998
UTS-1	74.581	13.247	1.003	2.254	3.529	0.605	1.335	1.204	-	0.205	0.206	0.020	0.60	98.789
UTS-2	67.355	18.409	0.681	3.188	5.453	0.835	0.817	2.124	0.089	0.110	0.134	-	0.80	100
UTS-4	62.413	15.343	0.557	2.395	5.115	0.585	10.229	1.504	0.830	-	-	0.024	1.00	100
UTS-7	71.201	16.585	0.248	2.503	4.741	0.547	0.978	1.929	-	-	-	0.019	1.20	100.001

Table 3. Correlation matrix of different oxides of sandstone, Tipam Sandstone Formation.

	SiO <sub>2</sub>	Al <sub>2</sub> O <sub>3</sub>	Na <sub>2</sub> O	K <sub>2</sub> O	Fe <sub>2</sub> O <sub>3</sub>	TiO <sub>2</sub>	CaO	MgO	MnO	P <sub>2</sub> O <sub>5</sub>	BaO	ZrO <sub>2</sub>
SiO <sub>2</sub>	1.000	.435	.241	.185	-.275	-.354	-.937**	-.502	-.839**	.041	.083	-.594
Al <sub>2</sub> O <sub>3</sub>		1.000	-.599*	.854	-.026	-.016	-.650**	-.667**	-.665*	-.421	-.438	-.519
Na <sub>2</sub> O			1.000	-.569*	-.136	-.002	-.051	.330	-.101	0.37	.233	3.14
K <sub>2</sub> O				1.000	-.032	.164	-.415	-.341	-.438	-.622	-.193	-.530
Fe <sub>2</sub> O <sub>3</sub>					1.000	.283	.038	-.106	.008	.318	.110	.413
TiO <sub>2</sub>						1.000	.213	.301	-.085	-.042	.096	.725*
CaO							1.000	.608*	.870*	.063	.160	.713
MgO								1.000	.605	-.233	.055	.461
MnO									1.000	.565	.530	.132
P <sub>2</sub> O <sub>5</sub>										1.000	5.35	-0.81
BaO											1.000	-.452
ZrO <sub>2</sub>												1.000

\*\* Correlation is significant at the 0.01 level (2-tailed).

\* Correlation is significant at the 0.05 level (2-tailed).

the maximum value of 8.1 wt% and the minimum value of the 5.3 wt% with an average of 6.6 wt%. The TiO<sub>2</sub> content ranges from 0.6 to 1.1 wt% with average of 0.9 wt% for the shale samples. It shows negative correlation with MgO (r = -0.82). CaO varies from 0.8 to 44.7 wt%, with an average of 8.9 wt% of the shale samples. It shows high positive correlation with MnO (r = 0.99) and P<sub>2</sub>O<sub>5</sub> (r = 0.90). The MgO content varies from 2.5 to 16.3 wt% with an average of 5.3 wt%. MnO shows low contents with maximum value of 2.0 wt% and minimum 0.1 wt% with an average of 0.6 wt%.

## Discussion

### 1. Provenance

In general, geochemical approaches are equally applicable to coarse and fine-grained sedimentary rocks. This is not compatible with petrographical approaches where provenance studies for fine-grained as well as very coarse-grained sediments is difficult (McLennan *et al.*, 1993). There is growing evidence that even intimately associated sands and muds may be derived from quite different sources with different sedimentary histories and so both require their evaluation (e.g., McLennan *et al.*, 1990). Major

Table 4. Chemical composition (wt %) of shale, Tipam Sandstone Formation.

SAMPLE NO	SiO <sub>2</sub>	Al <sub>2</sub> O <sub>3</sub>	Na <sub>2</sub> O	K <sub>2</sub> O	Fe <sub>2</sub> O <sub>3</sub>	TiO <sub>2</sub>	CaO	MgO	MnO	P <sub>2</sub> O <sub>5</sub>	BaO	ZrO <sub>2</sub>	Loss	Total
MTS-2	51.336	16.091	0.299	2.615	6.410	0.979	17.173	3.054	0.970	0.273	-	-	0.80	100
MTS-3	61.863	20.609	0.505	3.788	6.572	1.042	0.917	2.489	0.072	0.189	0.133	0.022	1.80	100.001
MTS-4	62.212	19.152	0.596	3.031	6.268	1.009	2.964	2.994	-	0.216	0.134	0.021	1.20	99.768
MTS-5	63.919	19.076	0.505	3.371	5.761	1.051	1.006	2.505	-	0.151	-	0.026	1.60	98.631
UTS-3	63.149	19.055	0.614	3.433	6.464	1.046	1.458	2.805	0.078	0.164	0.168	0.017	1.40	99.799
UTS-5	61.585	19.716	0.570	3.433	8.097	1.030	0.831	3.115	0.088	0.129	0.139	0.021	1.00	99.754
UTS-6	53.390	13.416	0.346	2.003	7.719	0.708	1.898	16.253	0.094	0.139	0.108	-	3.40	98.846
UTS-8	27.804	7.400	0.230	1.229	5.338	0.589	44.740	8.913	1.984	0.326	-	-	1.00	99.553

Table 5. Correlation matrix of different oxides of shale, Tipam Sandstones Formation.

	SiO <sub>2</sub>	Al <sub>2</sub> O <sub>3</sub>	Na <sub>2</sub> O	K <sub>2</sub> O	Fe <sub>2</sub> O <sub>3</sub>	TiO <sub>2</sub>	CaO	MgO	MnO	P <sub>2</sub> O <sub>5</sub>	BaO	ZrO <sub>2</sub>
SiO <sub>2</sub>	1.000	.958**	.857**	.908**	.407	.880**	-.964**	-.483	-.950**	-.798	.821	.303
Al <sub>2</sub> O <sub>3</sub>		1.000	.859**	.798**	.329	.959**	-.871**	-.676	-.836*	-.659	.642	.085
Na <sub>2</sub> O			1.000	.846**	.267	.794*	-.776*	-.576	-.794	-.667	.849	-.830
K <sub>2</sub> O				1.000	.253	.954**	-.806*	-.730*	-.777	-.626	.685	.026
Fe <sub>2</sub> O <sub>3</sub>					1.000	.152	-.568	.263	-.766	-.682	-.443	-.333
TiO <sub>2</sub>						1.000	-.732*	-.827*	-.666	-.492	.776	.194
CaO							1.000	.240	.995**	.894**	-.214	-.242
MgO								1.000	.128	-.001	-.742	-.488
MnO									1.000	.944**	-.576	-.047
P <sub>2</sub> O <sub>5</sub>										1.000	.134	-.119
BaO											1.000	-.986*
ZrO <sub>2</sub>												1.000

\*\* Correlation is significant at the 0.01 level (2-tailed).

\* Correlation is significant at the 0.05 level (2-tailed).

element data can provide information on both the provenance composition and the effects of sedimentary processes, such as weathering and sedimentary sorting (McLennan *et al.*, 1993). It is recognized that sediment compositions have characteristics of certain assemblages of igneous/metamorphic/sedimentary source rocks that have specific styles of sedimentary history (e.g. Dickinson, 1985, 1988). The provenance types do not precisely correspond to those recognized from petrographical approaches but instead provide a different perspective of the plate tectonic association (McLennan *et al.*, 1993). So, bulk chemical composition is one of the major factors in characterizing the provenance types. The analyzed sandstones are characterized by higher ratios of SiO<sub>2</sub>/Al<sub>2</sub>O<sub>3</sub>. The maximum value is obtained from sample LTS-7 (6.3) and the lowest value from sample LTS-1 (3.3), with an average of 4.1. Shale samples are also characterized by higher value of SiO<sub>2</sub> and Al<sub>2</sub>O<sub>3</sub> contents are suggestive of decent felsic phases

for the provenance. The K<sub>2</sub>O/Na<sub>2</sub>O also shows high ratios both for sandstone and shale. The maximum values attain for the sandstone sample LTS-1 (27.8) and lowest value in LTS-10 (2.0). The average value of K<sub>2</sub>O/Na<sub>2</sub>O is 6.5 for sandstone and 6.3 for shale. Chemical Index of Alteration (CIA) values are also calculated for both sandstone and shale samples. CIA has been established as a general guide to the degree of weathering (Nesbitt and Young, 1984), although chemical changes resulting from other processes such as diagenesis and metamorphism have not been fully evaluated. Using molecular proportion CIA is shown as follows;  $CIA = Al_2O_3 / [Al_2O_3 + K_2O + Na_2O + CaO] \times 100$  or abbreviating,  $CIA = A / [A + K + N + C] \times 100$ . However 3 sandstone samples (LTS-6, LTS-8, and UTS-4) and 2 shale samples (MTS-2, UTS-8) show high values of CaO. In the calculation of CIA for sandstone and shale, CaO is calculated as only residing in silicates minerals. But the values of CaO for those 5 samples are much higher concentration due to the post

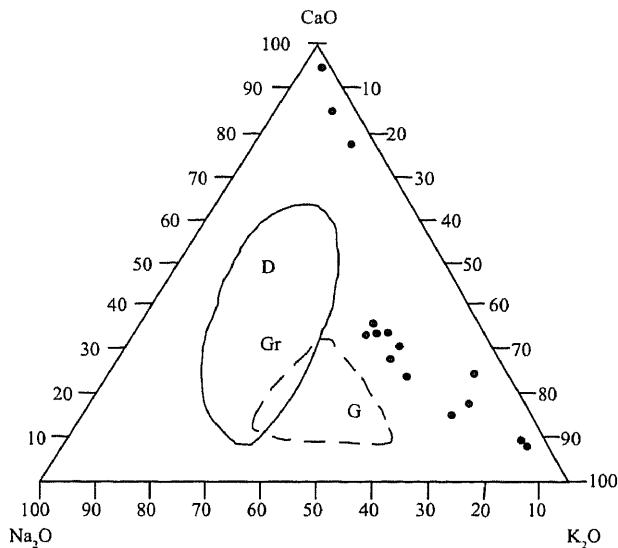


Fig. 2 CaO-Na<sub>2</sub>O-K<sub>2</sub>O plots for the sandstones of the Tipam Sandstone Formation. Boundaries are after Le Maitre (1976). (D = dacite, Gr = granodiorite, G = granite).

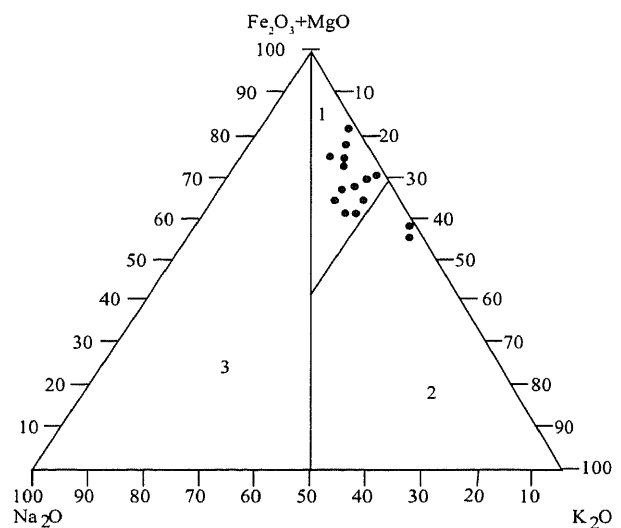


Fig. 3 (Fe<sub>2</sub>O<sub>3</sub>+MgO)-Na<sub>2</sub>O-K<sub>2</sub>O plots showing the relation of major oxide for the sandstones of the Tipam Sandstone Formation. Boundaries are after Blatt *et al.* (1980). (1 = ferromagnesian-potassic sandstone, 2 = potassic sandstone, 3 = sodic sandstone).

depositional changes within the sediments. So, these 5 samples are to be avoided. Therefore the CIA value for the sandstone ranges from 71 to 87 with an average of 78, whereas those for shale from 74.4 to 80.3 with an average of 78. Usually the CIA values increase due to the increase in the degree of weathering. So, the value of CIA for sandstone and shale is moderate to higher.

Therefore, higher value of SiO<sub>2</sub>/Al<sub>2</sub>O<sub>3</sub>, K<sub>2</sub>O/Na<sub>2</sub>O and CIA of sandstone and shale reflects a dominance of upper crustal granitic sources (e.g., Singo granite, Uganda from Nagudi *et al.*, 2003) and a relatively severe weathering (and recycling) history (McLennan *et al.*, 1993). So, the provenance is regarded as old upper continental crust (OUC). They include old stable cratons and the old continental foundation of active tectonic settings that contains recycled sedimentary and metasedimentary rocks. This type of provenance component constitutes old igneous, metamorphic and sedimentary terranes that have been influenced by intracrustal geochemical fractionation which include process of both intracrustal partial melting and or crystal fractionation (McLennan *et al.*, 1993). The geochemistry of sediments derived from these terranes are normally characterized by relatively consistent compositions, reflecting a broad and well mixed provenance (Potter, 1978) and the greater level of recycling expected for such environments (Veizer and Jansen, 1979, 1985).

Triangular plot of CaO, Na<sub>2</sub>O and K<sub>2</sub>O of the sandstone for focusing source rocks may be granite in

nature (after Le Maitre, 1976) (Fig. 2), because most data are concentrated in the vicinity of the granite field. But three samples placed on the top of the diagram due to the high amount of CaO in the sediment caused by post depositional changes within the sediments. According to Blatt *et al.* (1980) (Fe<sub>2</sub>O<sub>3</sub>+MgO)-Na<sub>2</sub>O-K<sub>2</sub>O triangular plot reveals that the sandstone samples are largely restricted to the ferromagnesian-potassic sandstone (Fig. 3). In the variation diagram Fe<sub>2</sub>O<sub>3</sub>-MgO-TiO<sub>2</sub> (after Condie, 1967), the geochemical data of sandstones fall near the fields of granite and quartz-monzonite (Fig. 4). Another approaches (Condie, 1967) for plotting the geochemical data of sandstones on the variation diagram (CaO-Na<sub>2</sub>O-K<sub>2</sub>O) indicates that most of the source rock may be granite and monzonite (Fig. 5). Only three data show the affinity near the basalt and andesitic zone, due to the increase of CaCO<sub>3</sub> within the sediment due to post depositional changes.

Harker variation diagrams of sandstone samples (Fig. 6) show that the positive correlation exists between SiO<sub>2</sub> with K<sub>2</sub>O, Na<sub>2</sub>O and Al<sub>2</sub>O<sub>3</sub> whereas negative correlation exists between SiO<sub>2</sub> with CaO, Fe<sub>2</sub>O<sub>3</sub> and MgO. So the concentration of K<sub>2</sub>O and Na<sub>2</sub>O increases with increasing SiO<sub>2</sub> whereas the concentration of CaO, Fe<sub>2</sub>O<sub>3</sub> and MgO decreases with increasing SiO<sub>2</sub> concentration. It seems that the derivation of the sediment from the felsic igneous fields i.e. from the granite rock, because SiO<sub>2</sub> contents

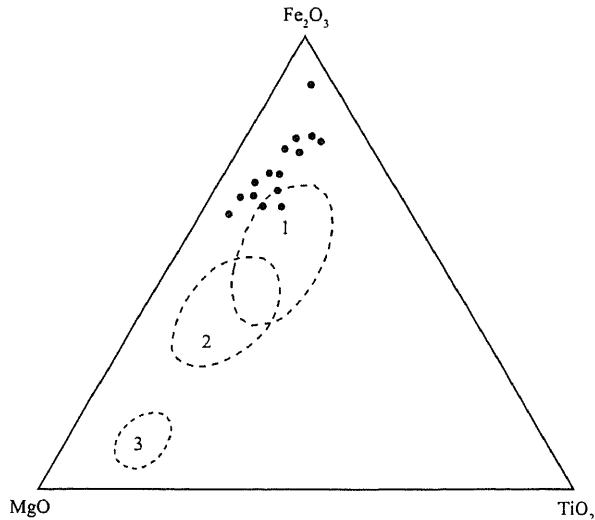


Fig. 4  $\text{Fe}_2\text{O}_3$ - $\text{MgO}$ - $\text{TiO}_2$  diagram (after Condie, 1967) showing the plots of sandstones of Tipam Sandstone Formation. (1. granite and quartz-monzonite, 2. quartz diorite and granodiorite, 3. basalt).

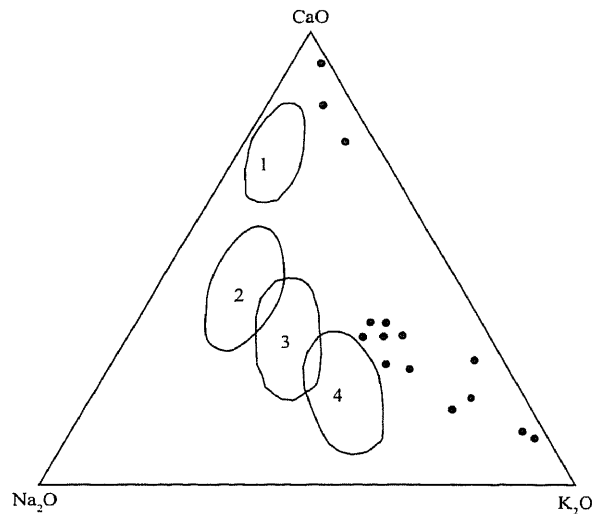


Fig. 5  $\text{CaO}$ - $\text{Na}_2\text{O}$ - $\text{K}_2\text{O}$  diagram (after Condie, 1967) showing the plots of sandstones of Tipam Sandstone Formation. (1. basalt and andesite, 2. quartz diorite, 3. granodiorite, 4. granite and monzonite).

are relatively high (mostly 60–76%).

From above observations, the geochemical characteristics reveal that higher values of  $\text{SiO}_2/\text{Al}_2\text{O}_3$ ,  $\text{K}_2\text{O}/\text{Na}_2\text{O}$  and CIA of sandstone and shale indicate the dominance of old upper crustal granitic source, including recycled sedimentary rocks of the old continental foundation of active tectonic settings. Triangular plots of  $(\text{CaO}-\text{Na}_2\text{O}-\text{K}_2\text{O})$ ,  $(\text{Fe}_2\text{O}_3+\text{MgO})-\text{Na}_2\text{O}-\text{K}_2\text{O}$ ,  $(\text{Fe}_2\text{O}_3-\text{MgO}-\text{TiO}_2)$  and  $(\text{CaO}-\text{Na}_2\text{O}-\text{K}_2\text{O})$  highly recommend that the source rocks are granite and quartz-monzonite and the samples are largely restricted to the ferromagnesian-potassic sandstone.

## 2. Tectonic setting of depositional basin

The tectonic setting of the depositional basin of the Tipam Sandstone Formation is formulated on the basis of major oxides of sandstone and shale by plotting different chemical variables on different bivariate diagrams. Roser and Korsch (1986, 1988) utilized mudstone in their work, and developed discrimination to cover the full range of grain size from sand to mud. In this study, geochemical data (major oxides) of both sandstone and associated shale (mudstone) have been applied to discriminate the tectonic setting of the depositional basin. Sandstone and mudstone of different tectonic setting are characterized by different chemical characteristics (major oxides). The different chemical parameters are used to evaluate the tectonic setting of the depositional basin. Major element geochemistry gives clues to the provenance

types as well as weathering condition, both of which are controlled by the tectonic setting of the basin. Influence of diagenesis also depends on the tectonic setting of the area (Siever, 1979).

$\text{SiO}_2$  content versus  $\text{K}_2\text{O}/\text{Na}_2\text{O}$  (Fig. 7) as well as  $\text{SiO}_2/\text{Al}_2\text{O}_3$  versus  $\text{K}_2\text{O}/\text{Na}_2\text{O}$  (Fig. 8) of sandstones and shales are used to discriminate tectonic setting (Roser and Korsch, 1986). Most of the data fall into the passive margin (PM) field. In the former diagram only three data fall within the active continental margin (ACM) boundary, being due to the higher amount of  $\text{CaCO}_3$ , the post depositional changes within the sediments. LTS-6 sample is to be avoided due to its very high content of  $\text{CaCO}_3$ . In the case of later diagram (Fig. 7), however, all the data of sandstone and shale fall into the passive margin field. According to Roser and Korsch (1986), PM sediments are largely quartz-rich sediments derived from plate interiors or stable continental areas and deposited in intracratonic basin or on passive continental margins. The geochemical characteristics of both sandstones and shales positively support it.

Many authors (Middleton, 1960; Crook, 1974; Maynard *et al.*, 1982; Bhatia, 1983) proposed that if the ratio of  $\text{K}_2\text{O}/\text{Na}_2\text{O}$  is greater than unity ( $\text{K}_2\text{O}/\text{Na}_2\text{O} > 1$ ), a passive margin tectonic margin is supported for the sediments. Because that the value of  $\text{K}_2\text{O}/\text{Na}_2\text{O}$  is greater than unity for sandstone samples in this study. The sediment could be deposited in a basin along passive margin tectonic setting, which includes rifted

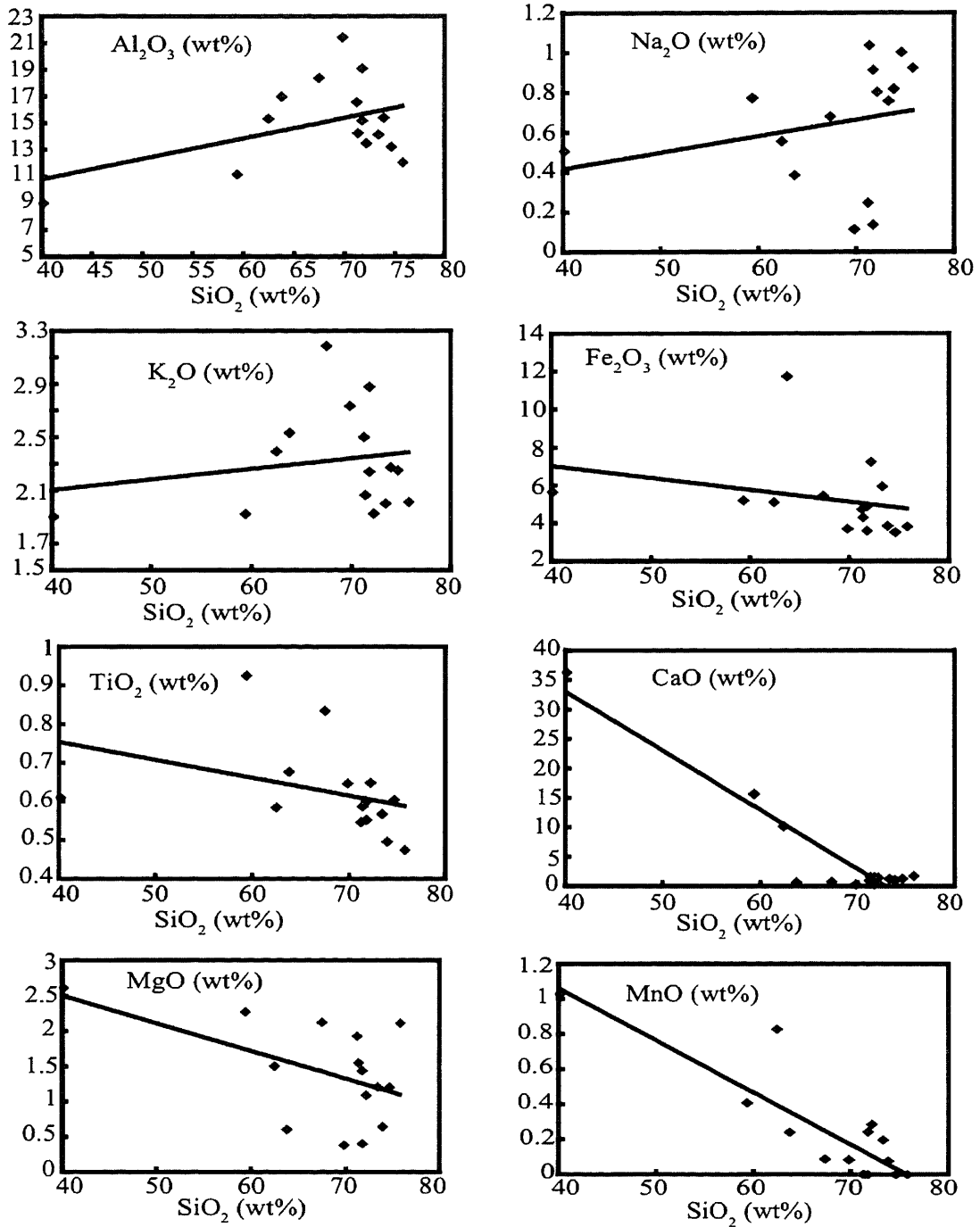


Fig. 6 Harker variation diagram of major elements for Sandstone of Tipam Sandstone Formation.

continental margin, intracratonic and rift bounded basins. Plots of some geochemical parameters in different bivariate diagrams  $K_2O/Na_2O$  vs.  $SiO_2$  and  $SiO_2/Al_2O_3$  vs.  $K_2O/Na_2O$  (Rosier and Korsch, 1986) and  $K_2O/Na_2O$  ratio highly supports that the deposition of Tipam Sandstone occurred in a basin along passive continental margin setting (Fig. 7).

### 3. Paleoclimate and weathering

The effects of variable degrees of weathering in source areas can be important in influencing alkali and alkaline earth element (AE) contents of terrigenous sedimentary rocks (Nesbitt *et al.*, 1980; Schau and Henderson, 1983; Reimer 1985; Granstaff *et al.*, 1986). The degree of chemical weathering is a function of

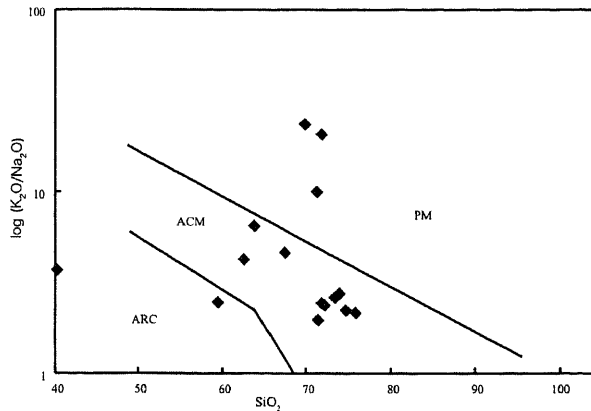


Fig. 7  $K_2O/Na_2O$ - $SiO_2$  relations of sandstones-mudstones of the Tipam Sandstone Formation. Boundaries are after Roser and Korsch (1986). (Abr. PM = passive margin, ACM = active continental margin, ARC = island-arc).

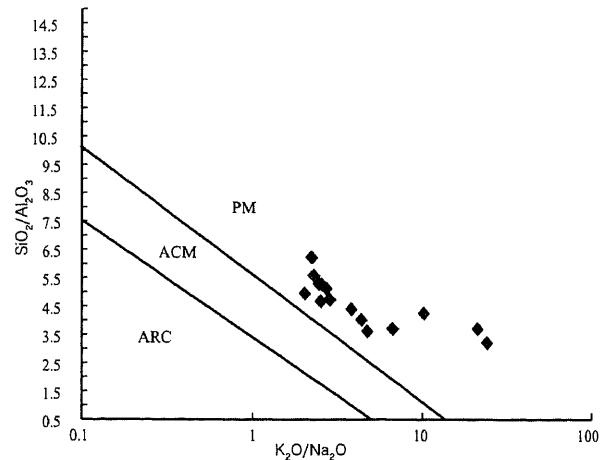


Fig. 8  $SiO_2/Al_2O_3$ - $K_2O/Na_2O$  relations of sandstones-mudstones of the Tipam Sandstone Formation. Boundaries are after Roser and Korsch (1986). (Abr. PM = passive margin, ACM = active continental margin, ARC = island-arc).

climate and erosion rate, the latter of which varies with the rate of tectonic uplift. The bulk chemical changes that take place during weathering have also been used to quantify the weathering history of sedimentary rocks, primarily to understand past climatic conditions (Nesbitt *et al.*, 1980; Nesbitt and Young, 1982, 1984). CIA value have been calculated for sandstone and shale samples. The CIA value for the sandstone ranges from 71 to 87 with an average of 78, whereas the CIA value for shale ranges from 74.4 to 80.3 with an average of 78. The CIA values increases due to the increase in the degree of weathering. Therefore, the value of CIA for sandstone and shale is moderately to highly suggest that the sediments were intense weathered in the source area. High values of  $SiO_2/Al_2O_3$  and  $K_2O/Na_2O$  of sandstone and shale also reflect relatively severe weathering (and recycling) history of the Tipam Sandstone Formation (McLennan *et al.*, 1993). This is also suggested by high concentration of  $TiO_2$ , which is generally known as immobile species. The maximum concentration of  $TiO_2$  attains for the sample LTS-8 (0.9 wt%) and the minimum concentration for the sample LTS-7 (0.5 wt%). The average concentration of  $TiO_2$  in the sandstone is 0.6 wt%. Therefore, the high concentration of  $TiO_2$  suggests that the sediment were subjected to intensive weathering in the source area. The concentration of  $Fe_2O_3$  in the sandstone sample is comparatively high. The maximum concentration is 11.8 wt% and minimum concentration is 3.5 wt%, with an average value of 5.3 wt%. This high concentration of iron is indicative of oxidation, hydration and leaching processes involved during weathering of the Tipam Sandstone Formation (Schau

and Henderson, 1983). Low contents of  $Na_2O$  (1 wt%) of sandstone and shale also indicate intensive to moderate weathering of the source rock. The ratios of  $SiO_2/(Al_2O_3+K_2O+Na_2O)$  (Suttner and Dutta, 1986) express the climatic condition during the deposition of the sediments in the basin. The plot in  $SiO_2$  vs.  $(Al_2O_3+K_2O+Na_2O)$  diagram for the 15 sandstone samples indicates that the sediments deposited in the basin under semi-arid climatic condition (Fig. 9). Because the maximum data clustering in the semi-arid climatic zone instead of humid climatic zone, alumina/kaolinite decomposition and partial feldspar decomposition in the sandstone might occur as a result of decomposition after deposition. The concentration of alumina is relatively high due to the decomposition of feldspar. But it is very much interesting to fit this concept with the upheaval of Himalaya and with Asian monsoon. Because several workers have carried out a lot of works on sedimentology and petrography of Tipam Sandstone (Johnson and Alam, 1991; Roy *et al.*, 2006; Roy, 2003), and they concluded that from facies analysis and mineral association the sediments were deposited under humid to semi-humid climatic condition.

Therefore, extensive mechanical weathering, abundant alumina, high concentration of  $TiO_2$  and iron that preserved in the ferric state, all indicate that the sediments in the source area were subjected by intensive weathering. The depositional conditions were under humid to semi humid climatic nature, because intensive weathering associated with mechanical and chemical disintegration that are related to the high

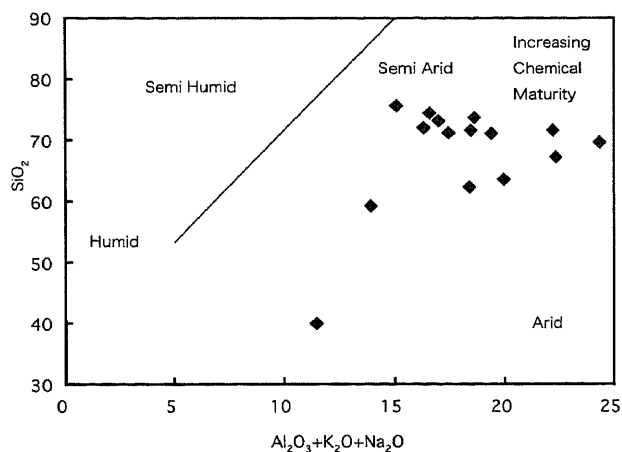


Fig. 9 Bivariate plots of SiO<sub>2</sub> (wt%) vs Al<sub>2</sub>O<sub>3</sub>+K<sub>2</sub>O+Na<sub>2</sub>O (wt%) to discriminate climatic condition during the deposition of the Tipam Sandstones (after Suttner and Dutta, 1986).

rainfall, significant tectonic upliftment and high rate of erosion might occur. Those are only possible under humid to semi humid climatic conditions.

### Conclusions

The sandstone samples are largely restricted to the ferromagnesian-potassic in nature. Harker variation diagrams support the derivation of sediment from felsic igneous field i.e from granite rock. Some variation diagrams, such as (CaO-Na<sub>2</sub>O-K<sub>2</sub>O), (Fe<sub>2</sub>O<sub>3</sub>-MgO-TiO<sub>2</sub>) and (CaO-Na<sub>2</sub>O-K<sub>2</sub>O) along with high values of SiO<sub>2</sub>/Al<sub>2</sub>O<sub>3</sub>, K<sub>2</sub>O/Na<sub>2</sub>O and CIA highly support that the source rocks were dominated by old upper crustal granite, quartz monzonite, including recycled sedimentary rocks of the old continental foundation of active tectonic settings. SiO<sub>2</sub> versus K<sub>2</sub>O/Na<sub>2</sub>O as well as SiO<sub>2</sub>/Al<sub>2</sub>O<sub>3</sub> versus K<sub>2</sub>O/Na<sub>2</sub>O diagrams of sandstones and shales along with K<sub>2</sub>O/Na<sub>2</sub>O ratio indicate that most of the sediment deposited in a basin along passive continental margin setting. The value of K<sub>2</sub>O/Na<sub>2</sub>O for sandstones being greater than unity also supports the tectonic setting. High value of SiO<sub>2</sub>/Al<sub>2</sub>O<sub>3</sub>, K<sub>2</sub>O/Na<sub>2</sub>O and low value of Na<sub>2</sub>O (1%) of sandstone and shale, and abundant alumina, high concentration of TiO<sub>2</sub> and iron that preserved in the ferric state, all suggest relatively severe weathering (and recycling) history of the Tipam Sandstone Formation.

From above observations it may be concluded that the sediments of Tipam Sandstone Formation seem to have been derived from the old upper crustal granite and quartz monzonite including recycled sedimentary rocks of the old continental foundation of the tectonic settings that deposited in a basin along passive

continental margin setting. They might be under humid to semi-humid climatic condition due to the severe and intensive weathering (and recycling) history in the source area.

### Acknowledgements

The Directors of the Soil Research Development Institute (SRDI), Rajshahi and the Glass and Ceramic Division of Bangladesh Council of Science and Industrial Research (BCSIR), Dhaka, Bangladesh kindly permitted to analyze the samples. Dr. Toshiaki Tsunogae, Earth Evolution Sciences, University of Tsukuba, Japan and teachers of the Department of Geology and Mining, University of Rajshahi provided help and suggestions to improve the manuscript. Authors gratefully acknowledge all of them.

### References cited

- Alam, M., 1989, Geology and depositional history of Cenozoic sediments of Bengal Basin of Bangladesh. *Palaeogeo. Palaeoclim. Palaeoeco.*, **69**, 125–139.
- Bhatia, M. R. and Crook, K. A. W., 1986, Trace element characteristics of greywacke and tectonic setting discrimination of sedimentary basins. *Contr. Mineral. Petrol.*, **92**, 181–193.
- Bhatia, M. R., 1983, Plate tectonic setting and geochemical composition of sandstones; *Jour. Geol.*, **91**, 611–627.
- Blatt, H. Middleton, G. and Murray. R., 1980, *Origin of Sedimentary rocks*, 2<sup>nd</sup> Ed. Prentice-Hall; New Jersey. p. 782.
- Condie, K. C., 1967, Geochemistry of early Precambrian Greywackes from Wyoming. *Grochim. Cosmochim. Acta*, **31**, 2136–2047.
- Crook, K. A. W., 1974, Lithogenesis and geotectonics: the significance of compositional variation in flysch arenites (graywackes), in modern and ancient geosynclinal sedimentation. *SPM Su*, **19**, 304–310.
- Dickinson, W. R., 1985, Interpreting provenance relations from detrital modes of sandstones; p. 333–361. In: Zuffa, G. G. (Ed.): *Provenance of Arenites*. Dordrecht-Boston-Lancaster. D. Reidel Pub. Co.
- Dickinson, W. R., 1988, Provenance and sediment dispersal in relation to paleo-tectonics, and paleogeography of sedimentary basins, in kleinspehn, K. L., and Paola, C., eds, *New perspectives in basin analysis*. *New Sprin. Vaerlag*, p. 3–25.
- Evans, P., 1964, The tectonic framework of Assam. *J. Geol. Soc. Ind.*, **5**, 80–96.

- Granstaff, D. E., Edelman, M. J., Foster, R. W., Zibinden, E. and Kimberley, M. M., 1986, Chemistry and mineralogy of Precambrian paleosols at the base of the Dominion and Pongola Groups, South Africa. *Precam. Res.*, **32**, 97–132.
- Hiller, K. and Elahi, M., 1984, Structural development and hydrocarbon entrapment in the Surma Basin, Bangladesh (northwest Indo-Burman fold belt): Singapore 5<sup>th</sup> Offsh. SW. Conf., p. 656–663.
- Hiscott, R. N., 1984, Ophiolitic source rocks for Taconic-age flysch: Trace element evidence. *Geol. Soc. Am. Bull.*, **95**, 1261–1267.
- Johnson, S. Y. and Alam, A. M. N., 1991, Sedimentation and tectonics of the Sylhet Trough, Bangladesh. *Geol. Soc. Am. Bull.*, **103**, 1513–1527.
- Khan, M. A. M., Ismail, M. and Ahmad, M., 1988, Geology and hydrocarbon prospects of the Surma Basin, Bangladesh. Seventh Offshore Southeast Asian Conf. Singapore, p. 364–378.
- Le Maitre, R. W., 1976, The chemical variability of some common igneous rocks. *Jour. Petrol.*, **17**, 589–637.
- Maynard, J. B., Valloni, R. and Yu, H. S., 1982, Composition of modern deep-sea sands from arc related basins. In: J. K. LAGGETT (ed.), *Trench forearc Geology: Sedimentation and tectonics on modern and ancient active plate margins*. *Geol. Soc. Lon.*, **10**, 551–561.
- McLennan, S. M., Hemming, S., McDaniel, D. K. and Hanson, G. N., 1993, Geochemical approaches to sedimentation, provenance and tectonics, In: M. J. Johnsson & A. Basu (eds.), *Processes Controlling the Composition of Sediments*. *Geol. Soc. Am. Spec.*, **284**, 21–40.
- McLennan, S. M., Taylor, S. R., McCulloch, M. T. and Maynard, J. B., 1990, Geochemical and Nd-Sr isotopic composition of deep sea turbidites: Crustal evolution and plate tectonic association. *Geochem. et Cosmochim. Acta*, **54**, 2015–2050.
- Middleton, G. V., 1960, Chemical composition of sandstones; *Geol. Soc. Am. Bull.*, **71**, 1011–1026.
- Nagudi, B., Koeberl, C. and Kurat, G., 2003, Petrography and geochemistry of the Singo granite, Uganda, and implications for its origin. *Jour. Afric. Earth Sci.*, **36** (1), 73–87.
- Nesbitt, H. W. and Young, G. M., 1982, Early Proterozoic climates and plate motions inferred from major element chemistry of laticies. *Nature*, **299**, 715–717.
- Nesbitt, H. W. and Young, G. M., 1984, Prediction of some weathering trends of plutonic and volcanic rocks based on thermodynamic and kinetic considerations. *Geochem. et Cosmochim. Acta*, **48**, 1523–1534.
- Nesbitt, H. W., Markovics, G. and Price, R. C., 1980, Chemical processes affecting alkalis and alkaline earths during continental weathering. *Geochem. et Cosmochim. Acta*, **44**, 1659–1666.
- Potter, P. E., 1978, Petrology and chemistry of modern big river sands. *Jour. Geol.*, **86**, 423–449.
- Reimann, K. U., 1993, *Geology of Bangladesh*. Gebrüder, Borntraeger, Berlin, Germany. p. 160
- Reimer, T. O., 1985, Rare earth element and suitability of shale as indicators for the composition of the Archean continental crust. *Neues. Jahr. Mineral. Abh.*, **152**, 211–223.
- Roser, B. P. and Korsch, R. J., 1986, Determination of tectonic setting of sandstone- mudstone suites using SiO<sub>2</sub> content and K<sub>2</sub>O/Na<sub>2</sub>O ratio. *Jour. Geol.*, **94**, 635–650.
- Roser, B. P. and Korsch, R. J., 1988, Provenance signatures of sandstone-mudstone suites determined using discriminant function analysis of major element data. *Chem. Geol.*, **67**, 119–139.
- Roy, D. K., 2003, Geochemical and Petrological characterization of the Tipam sandstone formation in the Hari River Section, Jaintiapur, Sylhet District, Bangladesh. M. Sc. Thesis, Department of Geology and Mining. Rajshahi University, Rajshahi, Bangladesh (Unpublished).
- Roy, D. K., Roy, M. K., Islam, M. S. and Rahman, M. A., 2006, Lithofacies and depositional environments of the Lower Tipam sandstone in the Hari river Section, Jaintiapur, Sylhet, Bangladesh. *Land. Sys. Eco. Stud.*, **29** (accepted).
- Schau, M. and Henderson, J. B., 1983, Archean chemical weathering at three localities on the Canadian Shield. *Precam. Res.*, **20**, 189–224.
- Siever, R., 1979, Plate tectonic control on diagenesis. *Jour. Geol.*, **87**, 127–155.
- Suttner, L. J. and Dutta, P. K., 1986, Alluvial sandstone composition and paleoclimate, I. Framework mineralogy. *Jour. Sedi. Petrol.*, **56** (3), 326–345.
- Uddin, A. and Lundberg, N., 1998, Cenozoic history of the Himalayan-Bengal system: Sand composition in the Bengal basin, Bangladesh. *Geol. Soc. Am. Bull.*, **110**, 497–511.
- Veizer, J. and Jansen, S. L., 1979, Basement and sedimentary recycling and continental evolution. *Jour. Geol.*, **87**, 341–370.
- Veizer, J. and Jansen, S. L., 1985, Basement and sedimentary recycling-2: Time dimension to global tectonics. *Jour. Geol.*, **93**, 625–643.